RSC Advances

ROYAL SOCIETY OF CHEMISTRY

www.rsc.org/advances

Interactions of the products of oxidative polymerization of hydroquinone as catalyzed by birnessite with Fe(hydr)oxides – an implication of the reactive pathway for humic substance formations

R.R. Chang[a], S.L. Wang[a], Y.T. Liu[b], Y.T. Chan[b], J.T. Hung[c*], Y.M. Tzou[b*], K.J. Tseng[b]

[a]Department of Agricultural Chemistry, National Taiwan University, Taipei 10617, Taiwan

[b]Department of Soil and Environmental Sciences, National Chung Hsing University, Taichung 40227, Taiwan

[c]Department of Horticulture, National Taitung Junior College, Taitung 95045, Taiwan

*Corresponding author:

Tel: 886-4-22840373 ext 4206; 886-89-226389 ext 6000

E-mail address: ymtzou@dragon.nchu.edu.tw; hung01@ntc.edu.tw

Abstract

Polyphenol polymerization (PP) catalyzed by MnO_2 is an important pathway of humification processes in soils. Due to lack of aliphatic carbons, the products of PP are considered humic substance-like materials (HQs), which are subject to adsorption by Fe(hydr)oxide upon their formations. However, effects of HQs interactions with Fe(hydr)oxide on humification processes receive less attentions. In the study, the hydroquinone was reacted with birnessite for 1 d (HQ-1). After removal of residual birnessite, the filtrates were incubated for another 7 and 20 days, denoted as HQ-7, and HQ-20, respectively. The spectroscopic analyses of HQ samples indicated that oxidative polymerization of hydroquinone occurred within 1 d. With increasing incubation time, the molecular structure of the resultant HQ continued to change and became increasingly similar to that of natural humic acid (HA) even in the absence of birnessite. Upon the adsorption of HQs to Fe(hydr)oxide, the changes in the IR absorption band indicated the complexation of HQ carboxyl groups with metals centers on the mineral surfaces. HQ-20 were preferentially adsorbed on Fe(hydr)oxides because it contained a higher number of carboxyl groups than the counterparts with a smaller molecular weight. In addition, the steric arrangements and the distributions of the adsorption sites on Fe(hydr)oxide, matching closely the structures of larger molecules, may also contribute to the preferential adsorption. This study imply that the HQ with a larger molecular size can be accumulated in soils while reacting with Fe(hydr)oxides during its formation, and the association of HQs with aliphatic carbons derived from Maillard reaction may contribute to humic substance (HS) formations.

Key words:

Humic acid; polyphenol polymerization; Fe(hydr)oxides; adsorption

Introduction

Humic substances (HSs) are comprised of humic acid, fulvic acid and humin, the major components of soil organic matter (SOM), are commonly found in surface soils, sediments and water.[1, 2] HSs are derived from the humification processes that transform organic precursors, such as sugars, polyphenols and amino compounds, to recalcitrant organic components in soils and sediments.[3, 4] In general, humic substances consist of various organic compounds that contain aliphatic moieties and oxidized aromatic components from lignin and polyphenols. The transformation from organic precursors to HSs in soil is usually driven through abiotic catalytic reactions, including Maillard reaction and polyphenol polymerization (PP). The Maillard reaction is a reaction between amino acids and reducing sugars under ambient conditions.[5, 6] Jokic et al.[3] found that the aliphatic structures could be produced during the polycondensation process between glycine and catechol while the Maillard regent (i.e. glucose) was added. On the contrary, the PP reaction results in an increase in the number of aromatic structures due to its higher degree of condensation via oxidative polymerization of polyphenol.[7] Because of the lack of aliphatic structures, the chemical compositions of PP products are different to those of HSs, which contain certain amounts of aliphatic molecules and recalcitrant residues of plants and algae.[8] Thus, we defined the products of PP as a humic substance-like material (HQ), which is distinct from HSs.[9]

As reported in the previous studies, minerals showed the promise to promote the PP reaction in soils. For example, Jokic et al.[3] found that clay minerals and metal oxides could promote the transformation of phenolic compounds to precursors of HSs through an oxidative polymerization reaction, including ring cleavage, decarboxylation, and/or dealkylation. Risser and Bailey[10] found that manganese oxides (e.g., birnessite, δ-MnO_2), existing in many soils and sediments, exhibited a stronger ability in the abiotic conversion of organic compounds than other metal oxides, such as of iron, aluminum, and silicon. Zherebker et al.[11] also reported that Mn(IV) oxides could enhance the oxidation of phenolic compounds, such as hydroquinone, over a pH range of pH 4-8 in soils. Shindo and Huang[12] indicated that HQs were produced within one day in the presence of MnO_2; however, our preliminary studies showed that the newly formed HQs were unstable because the absorbance of HQs changed continuously over a prolonged reaction time even in the absence of MnO_2. Because HQ is an important intermediate of humification processes, its interaction with soil minerals might influence the formation and stabilization of soil organic matter (SOM)

and control sustainable carbon cycling. In soils, it is well known that HSs might associate or form assemblages with minerals/metal oxides which would hinder the microbial decay and decomposition of the organic materials.[13-15] Regarding the HQ, however, its interactions with soil minerals have been rarely studies. Because Fe(hydr)oxides are widely distributed in soils and associated closely to MnO_2, contributions of Fe(hydr)oxides to the formations, accumulations, and conversions of HQs should be addressed more precisely to clarify the humification processes of organic matter in soils.

In humic acid extracted from a volcanic soil enriched with Fe(hydr)oxides, Chen et al.[16] and Huang et al.[17] found that larger molecular weights (MWs) of aromatic groups dominated the compositions of the humic acids. However, the humic acids extracted from a peat soil with less amounts of Fe(hydr)oxides showed a different distributions of MWs and aromaticity.[18] That is, the variances in chemical compositions of SOM are related to not only the origins of the source SOM[19, 20] but also the presence of specific soil minerals with high affinity to SOM. Because the PP reaction is considered a major abiotic pathway in converting organic precursors to HSs, the associations of PP products obtained at different stages with soil minerals may be helpful to preserve the labile substances against the microbial decay and benefit for subsequent humification. While previous studies gauged the magnitude of the PP processes, a complementary mechanistic study that provides the explanation such as the molecular structures and chemical compositions of HQs is still missing. Besides, to the best of our understanding, how Fe(hydr)oxides are involved and affect the humification of SOM through abiotic PP processes is still unclear. Thus, we aimed to determine the products of oxidative polymerization of hydroquinone with and without the catalysis of birnessite and investigate the adsorption kinetics of the HQs on Fe(hyd)oxides upon their formations. We speculated that the interactions of the HQs with Fe(hydr)oxides, such as ferrihydrite and goethite, may contribute diversities to the chemical compositions of SOM.

Experimental

Preparation of humic substance-like materials

The oxidative polymerization of hydroquinone by birnessite (δ-MnO_2) was carried out according to the procedures of Shindo and Huang[12] and Jokic et al.[3] Birnessite was prepared using the method of McKenzie [21]. Sodium acetate (0.1 M, 125 ml) containing 10 mM hydroquinone (Sigma, purity ≥ 99%) at pH 6 in a 500 ml flask

was mixed with 125 mg birnessite. The chemicals and reagents used in the study are all of analytical grade. The mixture suspension was incubated in an oscillating shaker in a water bath at 25 ^{o}C for 24 h and filtered using a 0.2 μm pore-size membrane filter. The solids on the filter were collected and analyzed using an X-ray diffractometer (PANalytical X'Pert Pro MRD) with Cu-Kα radiation. The XRD patterns were recorded from 2 to 80° 2θ with a scan rate of 2° 2θ min^{-1}. The filtrate was subsequently allowed to age under ambient conditions for 1, 7 and 20 days, respective. Then, the suspensions were collected, acidified to pH 1.0 using 6 M HCl to obtain the precipitates. The precipitates were centrifuged at 2,683 g for 30 min and transferred to dialysis tubing with a molecular weight (MW) cutoff of 3500 Da and dialyzed against deionized water until the electrical conductivity (EC) of the dialysate was < 50 μS cm^{-1}. The precipitates of humic substance-like material products, referred to as HQ-1, HQ-7, ad HQ-20, respectively, were then lyophilized and stored prior to uses.

Sample collection and extraction of HA from a volcanic soil

The volcanic soil, collected from the Yangming Mountain area (25N, 121°32'50" E), which represents a sample of soil that has been likely formed under the influences of Fe(hydr)oxides because the soil is enriched with Fe(hydr)oxides and contains larger MWs of HSs in the SOM. The Yangming mountain soil is classified as Andisol.[22] The physical and chemical properties of the volcanic soil can be referred to the reports of Huang et al.[23] and Chang et al.[24]. The major minerals in the volcanic soils include kaolinite, illite, quartz, gibbsite, chlorite, and high contents of Fe/Al non-crystalline mineral. The total organic carbon is 156 g kg^{-1}.

Extraction of the HA followed the standard procedure of the International Humic Substance Society (IHSS) as outlined by Swift [25]. Briefly, an aliquot (30 g, air-dried, passed through a 2 mm sieve) was treated with HCl (300 mL, 1 M) in a 500 mL centrifuge bottle. After shaking for 1 h, the suspension was centrifuged at 2,683 g for 20 min and the supernatant was decanted. The residue was re-suspended in NaOH (300 mL, 0.1 M, in a N_2 atmosphere) on a shaker for 24 h (25 ^{o}C). Following centrifugation, the supernatant was collected and acidified with 6 M HCl (to pH 1–2) to obtain the HA fraction.

Sample Characterization

UV-Visible spectroscopy

Prior to being acidified, the soluble HQ samples, formed in the presence or absence of birnessite, were examined using a UV-visible spectrophotometer (Varian,

Cary-50) over a wavelength range of 400-700 nm. The readings of the absorbance within the specific wavelength range were commonly used to examine the humification extent of HAs. [12, 26]

Elemental compositions

The elemental contents (C, H, O, and N) of HQ and HA precipitates were investigated by a Heraeus CHNOS Rapid F002 Elemental Analyzer.

Fourier Transform Infrared Spectroscopy (FT-IR)

FT-IR spectra of the original hydroquinone, HQ-1, HQ-7, HQ-20 and the HA samples were obtained using a Thermo-Nicolet Nexus FT-IR spectrometer in the range 4000-400 cm^{-1} with a resolution of 4 cm^{-1}. The samples were purged with dry N_2 gas for at least 10 min to remove atmospheric CO_2 and moisture prior to analysis. A precise quantity (1 mg) of each sample was mixed with 200 mg KBr powder, and the mixture was ground and compressed into a translucent sample disk. FT-IR spectra were obtained by co-addition of 64 individual scans.

High Performance Size Exclusion Chromatography (HPSEC)

HPSEC was used to investigate the changes in MW distributions of each HQ sample as compared to that of HA. The HQ and HA samples were dissolved in 0.1 M KOH prior to HPSEC analyses. The SEC system consisted of a high-pressure liquid chromatography pump (Varian, ProStar 210) and a UV detector (ProStar 320-UV–Vis Detector). A Phenomenex protein was used in the SEC column (BioSep-SEC-s2000). The mobile phase consisted of 2 mM phosphate and 10 mM NaCl solutions at pH 7.0. The flow rate was maintained at 1 mL min^{-1} and the samples were detected at 254 nm. This technique was also used to examine the preferential adsorption of specific portions of HQ samples upon reaction with Fe(hydr)oxides.

Gas Chromatography Mass Spectrometry (GC-MS)

A GC-MS technique was used to identify the molecular variations of HQ1 and HQ20 samples during PP reaction and the results were compared with that of hydroquinone, a precursor of PP reaction. GC-MS was performed with an Agilent 7890A gas chromatograph and an Agilent 5975C mass selective detector. A HP-5 silica column (30 m x 0.32 mm, 0.25 μm film thickness) was used, and operated with the following oven temperature program: 150 ^{o}C held for 6 min, rising at 3^{o}C/min to

300 ^{o}C, held for 15 min. Helium was the carrier gas at 1 mL min^{-1}. The splitless injection mode was utilized, mass spectra (2.35 scan s^{-1}) were recorded under electron ionization at 70 eV, and the compounds were assigned by comparing with the NIST Library.

Adsorption of HQs and HA onto Fe(hydr)oxides

Fe(hydr)oxide preparation

Two line ferrihydrite was synthesized by neutralizing a 0.1 M $Fe(NO_3)_3$ with 1M NaOH. Well-crystallized goethite (α-FeOOH) was prepared by rapidly adding 5 M KOH to 1 M $Fe(NO_3)_3$ under constant stirring. The suspensions were immediately diluted to a volume of 2 L with deionized water, transferred to a polyethylene flask and incubated in an oven at 70 ^{o}C for 60 h. Each synthesized mineral was washed thoroughly using deionized water and dialyzed against deionized water until free of Cl^-. The samples were stored as suspensions under refrigeration. Details of the procedures are outlined by Schwertmann and Cornell.[27] The random powder samples of ferrihydrite and goethite were analyzed using an X-ray diffractometer (PANalytical X'Pert Pro MRD).

Preparation of HQ/HA stock solutions

Stock solutions of HA and HQ samples were prepared by dissolving 2.0 g HA and 1.0 g HQs in an 1 L solution with 0.1 M KOH under continuous stirring overnight. After passing through a 0.2 μm pore-size membrane filter, the filtrate was stored in a refrigerator for further uses. The C contents of the stock solutions were verified using a multi-N/C total organic carbon (TOC) analyzer (Analytik Jena, 2100).

Adsorption kinetics

Stocks of ferrihydrite and goethite suspensions were dispersed in an ultrasonic bath for 30 min and stirred constantly for 1 h. An appropriate volume of the suspension was extracted from each sample, transferred to a 50 mL centrifuge tube, and maintained at pH 4.0 using KOH (0.01 M) or HCl. An appropriate quantity of HA and HQ stock solution was added to the suspension to bring the final volume to 40 mL and the HA and HQ concentration of 30 and 50 mg C L^{-1} for goethite and ferrihydrite, respectively. The final suspension density for ferrihydrite and goethite was 0.25 and 0.62 g L^{-1}, respectively. The adsorption experiments were carried out on a rotary shaker, and the tubes were removed periodically. The suspensions were passed through 0.2 μm

pore-size membrane filters prior to being analyzed colorimetrically at 254 nm. Changes in the absorbance of HA or HQs after interacting with the solids were attributed to adsorption. A linear calibration curve of the absorbance measured by UV/Vis versus C mass determined by TOC was obtained, and thus, the absorbance could be readily converted to the C mass. The HA and HQ adsorption was expressed in units of mass of C per gram adsorbents.

Results and discussion

UV-Visible spectroscopy

The time-dependent absorbance changes in the products of PP reactions were examined via wavelength scan of the filtrate from 400 to 700 nm (Fig. 1), a rapid method to determine the degree of humification.[12] The absorbance increased slightly with incubation time, indicating that the oxidative polymerization of hydroquinone occurred slowly in the absence of Mn oxides (Fig. 1a). Addition of Mn oxide could accelerate the oxidative polymerization of hydroquinone as evidenced by a rapid increase of maximum absorbance at 400 nm (Fig. 1b). These results are consistent with the reports of Shindo and Huang,[12] showing that the colored (browning) reaction occurred within 1 d incubation. In this study, however, a continuous increase in absorbance was observed with increasing incubation time up to 20 days after filtering out MnO_2 (Fig. 1b), demonstrating that the polymerization reactions proceeded even after the oxidant (i.e., birnessite) was removed (Fig. 1b).

FT-IR spectroscopy

Infrared spectra of the reaction products (i.e., HQ-1, HQ-7, HQ-20), HA from a volcanic soil, and pure hydroquinone, were shown in Fig. 2a. Compared with the spectra of the HQs (Fig. 2b), hydroquinone exhibited more characteristic absorption bands in the fingerprint region. The bands at 3220, 3030 and 1517/1475 cm^{-1} were assigned to the OH, C-H and C=C stretching, respectively, on the single aromatic ring. The bands at 1209/1096 and 827/760 cm^{-1} were attributed to C-O stretching and C-H out-of-plane bending, respectively.[28]

Compared the absorption bands of hydroquinone with those from HQ-1 revealed that the intensities of the major hydroquinone bands became weaker, or disappeared as the result of Mn oxide additions, which gave rise to the oxidative polymerization reaction (Fig. 2a). The broad band at 3420 cm^{-1} was assigned to OH stretching, and the bands at 1720 and 1609 cm^{-1} were attributed to the asymmetric

stretching of COOH and the stretching of the H-bonded C=O of carbonyl groups, respectively (Fig. 2a). The presence of these two bands in the spectrum of HQ-1 indicated the OH group of hydroquinone was oxidized by Mn oxide to the COOH and C=O groups. Besides, the hydroquinone conjugated C=C modes at 1475 and 1517 cm^{-1} shifted to 1450 and 1500 cm^{-1}, respectively, upon oxidation (Fig. 2b). These changes in the spectra of major absorption peaks indicated the structural differences between hydroquinone and HQ-1.[3, 14]

HQ-7 and HQ-20 exhibited analogous spectra; nonetheless, a significant increasing in the band intensity at 1720 cm^{-1}, attributed to the asymmetric C=O stretching of COOH, was observed when the incubation period was extended to 20 days (Fig. 2b). An increase in the band intensity from -COOH groups indicated that the oxidative reaction continued, most likely because of the oxidation of OH or ether groups in the compounds with phenolic/alcoholic or aryl ether groups. Thus, the band at 1250 cm^{-1}, assigned to C–O stretching of aryl ethers, gradually decreased (Fig. 2b). In addition to the enhancement of carboxylic groups, the bands at 1550, 1450 and 1050 cm^{-1}, attributed to C-C stretching, disappeared when incubation time was extended (Fig. 2b). The occurrence of aromatic ring cleavage and re-polymerization of the aliphatic fragments may have caused the disappearance of these characteristic bands of HQ-20 sample. The spectra for HQ-20 and the HA showed distinct differences at 2905, 2849 and 1050 cm^{-1}, corresponding to C-C/C-H streching. These bands presented only for the HA sample, suggesting that the products synthesized from HQs lacked aliphatic C and differed significantly in chemical compositions from the HAs, which contained both aromatic and aliphatic domains.[23] Furthermore, the elemental analyses of HQ samples showed lower H/C atomic ratio values than HA, indicating that the HA was more aliphatic than the HQ samples, consistent with the FTIR results (Table 1).

HPSEC investigation of HQ samples

HPSEC was used to further investigate the effect of incubation time on the changes in the MW of HQs. The HPSEC elution curves of HQ-1, HQ-7, HQ-20, and HA were shown in Fig. 3. Two of the main and distinct distributions could be observed for the HA sample, and a wider multi-modality was observed for all the HQ samples (Fig. 3). HQ-1exhibited a longer retention time, incidating the presence of small molecules. Oxidiative polymerization during the extended incubation time led to a shift in the HQ absorption peak to a shorter retention time, particularly for HQ-20 (Fig. 3). This suggested that HQ-20 contained molecules larger than those in HQ-1 and HQ-7.

Although the HPSEC exhibited an intrinsic limitation of determining precisely the MWs of HQ/HA due to the lack of a suitable standard with similar structures to that of HQ/HA, the technique may be still feasible to describe qualitatively the changes in the apparent MWs of HQ/HA. Combined with the corresponding FTIR results, the results of HPSEC further demonstrated that oxidative polymerization of hydroquinone occurred with a longer incubation time.

GC-MS investigation of HQ samples

To investigate the products of the oxidative polymerization of hydroquinone, HQ-1, HQ-20, and hydroquinone samples were selected and examined using GC-MS, and the results were shown in Fig. 4 and Fig. 5. The appearance of larger organic fragments, such as the peaks at 8.912, 11.766 and 12.757 min with major m/z (mass-to-charge) ratios of 253-342 in the spectra after 1 day of reaction between hydroquinone and birnessite suggested the occurrence of oxidative polymerization reactions (Fig. 4). The spectra from HQ-1 showed some small MS fragments at 3.250, 4.717 and 5.982 min (Fig. 4 and Table 2), which may be the oxidative products or the derivatives of oxidative products of hydroquinone, such as para-benzoquinone, during ionization reactivity of mass analyses. However, these fragments disappeared for HQ-20, indicating a continuous polymerization or re-arrangement of the structures of HQ-1 with a prolonged incubation time even though the birnessite was removed after 1 day of reaction (Fig. 5). Although the structures of HAs are more complex than those of the HQ samples, [29-31] the fragmentation patterns in the mass spectra of HQ-20 sample were similar to those of natural HA (compared Fig. 5c with Fig. 5d). This suggested that the progressive polymerizations of HQ-1 would produce larger molecular structures, which possessed the ionization properties of HA, i.e., resisting the formations of charged molecules or molecule fragments upon mass analyses. Thus, the major fragments of 8.912, 11.766 and 12.757 min in the mass spectra of HQ-20 and HA samples exhibited relatively weak peak intensities as compared with those of HQ-1 (Fig. 4). The results corresponded with the reports of Gao et al.[32] who proposed that bisphenol A would form dimer products via hydroxylation and dealkylation in the presence of MnO_2.

Accordingly, the results of FT-IR (Fig. 2), HPSEC (Fig. 3), and GC-MS (Fig. 4, 5) spectra/curves indicated that, in the absence of birnessite, long term incubation allowed further conversion of HQ-1 to form compounds (i.e., HQ-20) with larger MWs and distinct chemical properties. Additionally, the XRD patterns of the MnO_2

treated with hydroquinone revealed that the characteristic peaks (7.15, 3.60, 2.44 A) of birnessite disappeared gradually with reaction time (Fig. 6), accompanied with the appearances of the peaks of $MnCO_3$ (3.07, 2.76, 2.47, 2.36 A). This result indicated that birnessite was transformed (reduced) to rhodochrosite upon hydroquinone oxidation. Because the Fe-containing minerals, such as ferrihydrite and goethite, associate intimately with Mn oxides and are widely distributed in soils, their interactions with HQs should be investigated to clarify the possible role of Fe(hydr)oxides involved in the PP-related humification processes.

Interactions of HQs and of HA with Fe(hydr)oxides

The adsorption kinetics of HA and HQs on ferrihydrite and goethite were shown in Fig. 7. Adsorption proceeded rapidly and reached a plateau within 20 min. The ferrihydrite and goethite demonstrated a similar adsorption order toward HQs and HA, i.e. HA > HQ-20 > HQ-7 > HQ-1. The adsorption of HQs and HA on ferrihydrite and goethite followed the second order kinetic model with a rate constant between 5.8×10^{-2} to 2×10^{-3} L mg^{-1} min^{-1} and between 2×10^{-4} to 7×10^{-5} L mg^{-1} min^{-1}, respectively (Table 3). Ferrihydrite exhibited a greater adsorption rate (particularly for HQ-20) and capacity than goethite due to its higher surface area and reactivity.

The time-dependent changes in the MW distributions of HQ-20 upon interaction with ferrihydrite were selected as a representative to investigate the changes in the molecular sizes of HQ-20 while contacting with Fe(hydr)oxides, and the results were shown in Fig. 8. A remarkable drop and disproportionate decrease in the presence of larger molecules occurred within a short retention time, particularly within the first one min (Fig. 8), which was attributed to the initial rapid adsorption of HQ-20 onto ferrihydrite (Fig. 7a). These results suggested that the adsorption of the larger organic molecules of HQ-20 on Fe(hydr)oxides was favorable. Due to a greater degree of polymerization, the steric arrangements and distributions of the adsorption sites on Fe(hydr)oxide may closely match the structure of larger molecule and hydrophobicity of HQ-20, leading to preferential adsorption. The phenomenon of preferential adsorption of specific organic moieties enriched with carboxyl groups on soil minerals was also observed by Balcke et al.[33], Hur and Schlautman[34], and Meier et al.[35]. Because HQ-20 contained more carboxyl groups than other HQ samples, the preferential adsorption of HQ-20 on Fe(Hydr)oxides was expected. FT-IR spectra of the ferrihydrite before and after interaction with HQ-20 showed that, upon adsorption of HQ-20 to ferrihydrite, the band at 1720 cm^{-1}, assigned to the asymmetric C=O

stretching vibration of COOH, disappeared (Fig. 9). In contrast, the band at 1609 cm^{-1}, attributed to the stretching of H-bonded C=O, weakened and shifted to 1575 cm^{-1}, indicating complexation with Fe-oxides. The band changes and shifts were consistent with the results of Gu et al.[36] and Kaiser and Guggenberger[14] who illustrated that a characteristic absorption of the carboxylate band occurred when this group interacted with Fe-oxides. Gu et al.[36, 37] and Parfitt et al.[38] suggested that the band shift from 1609 to 1575 cm^{-1} was due to complexation of carboxyl groups with metals on the mineral surfaces via a ligand exchange reaction.

Following the rapid interaction of HQ-20 with ferrihydrite, the adsorption rate of HQ-20 decreased slowly (Fig. 7a). Although the adsorption kinetics of HQs on Fe(hydr)oxide suggested that an apparent equilibrium could be reached within 30 min reaction (Fig. 7), the curve intensity of the HPSEC spectra changed continuously (Fig. 8). For example, during the stage of slow adsorption, the larger molecules in HQ-20 exhibited a preferential adsorption of ferrihydrite, as indicated by the gradual shift of the adsorption peaks toward a longer retention time in the HPSEC spectra when the reaction progressed (Fig. 8). The result suggested that adsorption of HQ-20 may proceed via structural rearrangement of the adsorption sites, which allowed adsorption of additional HQ-20 through molecule-molecule interaction or molecular diffusion into the interior of the adsorbent.

Based on the results, we developed a model to describe the humification processes with various scenarios under different environmental conditions. The findings and results in this study have brought new insights into the humification processes in soils, which have not been well understood before. The possible fates of HQs, produced from the oxidative polymerization of hydroquinone in the presence of MnO_2, in a soil profile as influenced by Fe(hydr)oxides were described in Fig. 10. Condition I illustrates the outcome of a strong leaching condition or in soils with limited Fe(hydr)oxides or other adsorptive minerals, allowing the small and polar fractions of HQs, formed at the early stages of oxidative polymerization of hydroquinone, to be distributed and moved rapidly throughout the environment. These hydroquinone-quinone intermediates may be leached out of the soil profile or interact with environmental contaminants, such as Cr(VI) and chlorophenol,[16, 23] and thus, the polymerization of quinones, leading to the formations of the precursor HS, becomes inhibited. In contrast, weak leaching conditions, illustrated for conditions II, cause the small fragments of HQs to be further polymerized and become associated with aliphatic compounds derived from Maillard reaction in soil solutions. Because

Fe(hydr)oxides preferentially adsorb the larger MWs of organic compounds, the biotic decompositions of quinones become inhibited, and thus, larger MWs of HSs can be accumulated in the SOM. The humic acid derived from Taiwanese volcanic soil, where the larger MWs of aromatic groups dominate the compositions of the humic acids, appears to resemble conditions II.[18] Finally, conditions III describes what happens under a limited amount of Fe(hydr)oxides in soils. In this case, organic compounds derived from quinones or Maillard reaction may be accessible and be partially degraded by microorganisms upon their formations, and thus, the MWs and aromaticity of humic acids exhibit more evenly distributed in the soils.[18]

However, the current scenario of describing the possible fates of HQs in the soil profiles are more appropriately applied when the HQs are produced with discrete or coated MnO_x prior to entering the soil pores with various amounts of Fe(hydr)oxides. On the other hand, co-existence of Fe(hydr)oxides and MnO_x either in discrete or associated phases may interfere with each other while interacting with hydroquinone. Besides, the reactions are greatly affected by the crystalline properties and the abundances (ratios) of the Fe(hydr)oxides and MnO_x as well as the exposed proportions of activated sites if the two minerals are strongly associated. Considering the complexity of a system with multi-minerals, influences of the mineral components on hydroquinone fate and subsequent humification processes under various environmental conditions merit alternative investigation.

Conclusions

Oxidative polymerization of hydroquinone catalyzed by birnessite can lead to the production of HQ within 24 h. The FT-IR, GC-MS and HPSEC analysis further proved that the oxidative polymerization proceeded continuously in the absence of birnessite up to 20 days. A significant increase in band intensity at 1720 cm^{-1} in the FTIR spectra resulted from the polymerization, which is attributed to the asymmetric C=O stretching of COOH. The results were most likely caused by the oxidation of hydroxyl or ether groups in functionalities such as phenolic/alcoholic or aryl ether. In addition, the GC-MS and HPSEC profiles indicated that larger molecules were formed after longer incubation time. The compositions of the HQs differed from those of the natural HA; however, the kinetic results suggested that the HQs/HA adsorption to either ferrihydrite or goethite followed a similar reaction mechanism. The steric arrangement and distribution of the absorption sites on Fe(hydr)oxide, which closely match the structures of larger molecules, may have led to the preferential adsorption of

higher MW of HQs/HA to these two adsorbents. In addition, larger molecular moieties in HQ/HA, with abundant carboxylic groups, the major adsorptive sites, contributed to the preferential adsorption. This study addresses that, in the absence of MnO_2, a slow process is involved for the conversion of simple aromatic compounds toward larger organic moieties in the PP reactions. This conversion may enhance the adsorptions of PP products to soil metal oxides, thereby preventing degradation by microbial attack, and thus, the aromatic-enriched C products from PP reactions can be sequestrated in soils with Fe(hydr)oxides. Thus, understanding the PP products at different stages and their interaction with soil minerals is helpful for clarifying the role of PP reactions in the productions of HS in soils.

Acknowledgements

The authors are deeply grateful for to the late P.M. Huang (University of Saskatchewan, Canada) for inspiration and M.H.B. Hayes (University of Limerick, Ireland) for invaluable suggestions which improved the manuscript. Thanks are also due to Yi-Chi Pao for her assistance in sample preparation. The work was financially supported by the National Science Council, ROC under project Nos. 101-2313-B-005-047-MY3 and 101-2621-M-005-005 and, in part, by the Ministry of Education, ROC under the Aim for Top University (ATU) plan.

References

1. M. H. B. Hayes and C. E. Clapp, *Soil Sci.*, 2001, **166**, 723-737.
2. A. Piccolo, *Soil Sci.*, 2001, **166**, 810-832.
3. C. Liu and P. M. Huang, *Org. Geochem.*, 2002, **33**, 295-305.
4. A. Jokic, M. C. Wang, C. Liu, A. I. Frenkel and P. M. Huang, *Org. Geochem.*, 2004, **35**, 747-762.
5. J. I. Hedges, in *Humic substances and their role in the environment*, eds. F. H. Frimmel and R. F. Christman, John Wiley and Sons, Chichester, UK, 1988, pp. 45-58.
6. J. Burdon, *Soil Sci.*, 2001, **166**, 752-769.
7. A. Y. Zherebker, D. Airapetyan, A. I. Konstantinov, Y. I. Kostyukevich, A. S. Kononikhin, I. A. Popov, K. V. Zaitsev, E. N. Nikolaev and I. V. Perminova, *Analyst*, 2015, **140**, 4708-4719.
8. F. J. Stevenson, *Humus Chemistry-Genesis, Composition, Reactions, 2nd edn* John Wiley and Sons, New York, NY, 1994.

9. S. Derenne and C. Largeau, *Soil Sci.*, 2001, **166**, 833-847.
10. M. H. B. Hayes and R. S. Swift, in *The Chemistry of Soil Constituents*, eds. D. J. Greenland and M. H. B. Hayes, Wiley, Chichester, 1978, pp. 179-320.
11. K. Kaiser and G. Guggenberger, *Org. Geochem.*, 2000, **31**, 711-725.
12. J. A. Baldock and J. O. Skjemstad, *Org. Geochem.*, 2000, **31**, 697-710.
13. R. G. Keil, D. B. Montlucon, F. G. Prahl and J. I. Hedges, *Nature*, 1994, **370**, 549-552.
14. J. A. Risser and G. W. Bailey., *Soil Sci. Soc. Am. J.*, 1992, **56**, 82-88.
15. H. Shindo and P. M. Huang, *Nature*, 1982, **298**, 363-3
16. S. Y. Chen, S. W. Huang, P. N. Chiang, J. C. Liu, W. H. Kuan, J. H. Huang, J. T. Hung, Y. M. Tzou, C. C. Chen and M. K. Wang, *Journal of Hazardous Materials*, 2011, **197**, 337-344.
17. S. W. Huang, P. N. Chiang, J. C. Liu, J. T. Hung, W. H. Kuan, Y. M. Tzou, S. L. Wang, J. H. Huang, C. C. Chen, M. K. Wang and R. H. Loeppert, *Chemosphere*, 2012, **87**, 587-594.
18. Y.-M. Tzou, S.-L. Wang, J.-C. Liu, Y.-Y. Huang and J.-H. Chen, *Journal of Hazardous Materials* 2008, **152**, 812-819.
19. B. S. Xing, *Environ. Pollut.*, 2001, **111**, 303-309.
20. B. S. Xing and J. J. Pignatello, *Environ. Sci. Technol.*, 1997, **31**, 792-799.
21. R. M. McKenzie, *Mineral Magazine*, 1971, **38**, 493-502.
22. Soil Survey, USDANRCS Agric. Handbook No. 436. US Gov. Print. Office, Washington, DC, 1999.
23. Y.-Y. Huang, S.-L. Wang, J.-C. Liu, Y.-M. Tzou, R.-R. Chang and J.-H. Chen, *Chemosphere*, 2008, **70**, 1218-1227.
24. R. R. Chang, R. Mylotte, M. H. B. Hayes, R. McInerney and Y. M. Tzou, *Naturwissenschaften*, 2014, **101**, 197-209.
25. R. S. Swift, in *Methods of soil analysis. Part 3. Chemical methods*, ed. D. L. S. e. al, Soil Science Society of America, American Society of Agronomy, Madison, WI, 1996, pp. 1018-1020.
26. Y. Chen, N. Senesi and M. Schnitzer, *Soil Sci. Soc. Am. J.*, 1977, **41**, 352-358.
27. U. Schwertmann and R. M. Cornell, *Iron oxides in the laboratory: Preparation and characterization*, VCH, Weinheim, 1991.
28. B. Sherine, A. J. A. Nasser and S. Rajendran, *Int. J. Eng. Sci. Tech.*, 2010, **2**, 341-357.
29. C. Xiaoli, T. Y. Shimaoka, G. Qiang and Z. Youcai, *Waste Manage*, 2008, **28**,

896-903.
30. X. Q. Lu, J. V. Hanna and W. D. Johnson, *Appl. Geochem.*, 2000, **15**, 1019-1033.
31. M. A. Olivella, J. C. d. Rio, J. Palacios, M. A. Vairavamurthy and F. X. C. d. l. Heras, *J. Anal. Appl. Pyrolysis*, 2002, **63**, 59-68.
32. N. Gao, Z. Yu, J. Hong, P. Peng and W. Huang, *Soil Sci.*, 2011, **176**, 265-272.
33. G. U. Balcke, N. A. Kulikova, S. Hesse, F.-D. Kopinke, I. V. Perminova and F. H. Frimmel, *Soil Sci. Soc. Am. J.*, 2002, **66**, 1805-1812.
34. J. Hur and M. A. Schlautman, *J. Colloid Interface Sci.*, 2003, **264**, 313-321.
35. M. Meier, K. Namjesnik-Dejanovic, P. A. Maurice, Y.-P. Chin and G. R. Aiken, *chemical Geology*, 1999, **157**, 275-284.
36. B. Gu, J. Schmltt, Z. Chen, L. Liang and F. McCarthy, *Environ. Sci. Technol.*, 1994, **28**, 38-46.
37. B. Gu, J. Schmitt, Z. Chen, L. Liang and J. F. McCarthy, *Geochim. Cosmochim. Acta*, 1995, **59**, 219-229.
38. R. L. Parfitt, A. R. Fraser and V. C. Farmer, *Soil Sci.*, 1977, **28**, 289-296.

Figure captions

Fig. 1. Effects of incubation time on the absorbance (400-700 nm) of filtrates obtained from the reaction of hydroquinone (a) without and (b) with birnessite at pH 6.

Fig. 2. (a) FT-IR spectra of HQ samples obtained after reactions for 1, 7 and 20 days, denoted as HQ-1, HQ-7 and HQ-20, respectively. HA from Yangming Mountain is provided for comparison. (b) Enlargement of 600-2000 cm^{-1} region.

Fig. 3. HPSEC elution curves of multi-modality of HQ-1, HQ-7, HQ-20 and HA.

Fig. 4. Total ion chromatogram of GC-MS spectra of hydroquinone and HQ samples obtained at 1 and 20 days, denoted as HQ-1 and HQ-20, respectively. HA is shown for comparison.

Fig. 5. 3D profile of GC-MS spectra of hydroquinone and HQ samples at 1 and 20 days, denoted as HQ-1 and HQ-20, respectively. HA is shown for comparison.

Fig. 6. XRD patterns of the solid residues obtained from the reactions of hydroquinone and birnessite at different reaction time.

Fig. 7. Adsorption kinetics of HA, HQ-20, HQ-7, and HQ-1 on (a) ferrihydrite and (b) goethite with a suspension density of 0.25 and 0.62 g L^{-1}, respectively, at pH 4 and 25 ^{o}C.

Fig. 8. Time-dependent changes of multi-modality of HQ-20 upon interaction with ferrihydrite.

Fig. 9. FT-IR spectra of HQ-20, ferrihydrite, and HQ-20-bearing ferrihydrite.

Fig. 10. The possible fate of hydroquinone in the soil profile developed at different environmental conditions with various Fe(hydr)oxide contents.

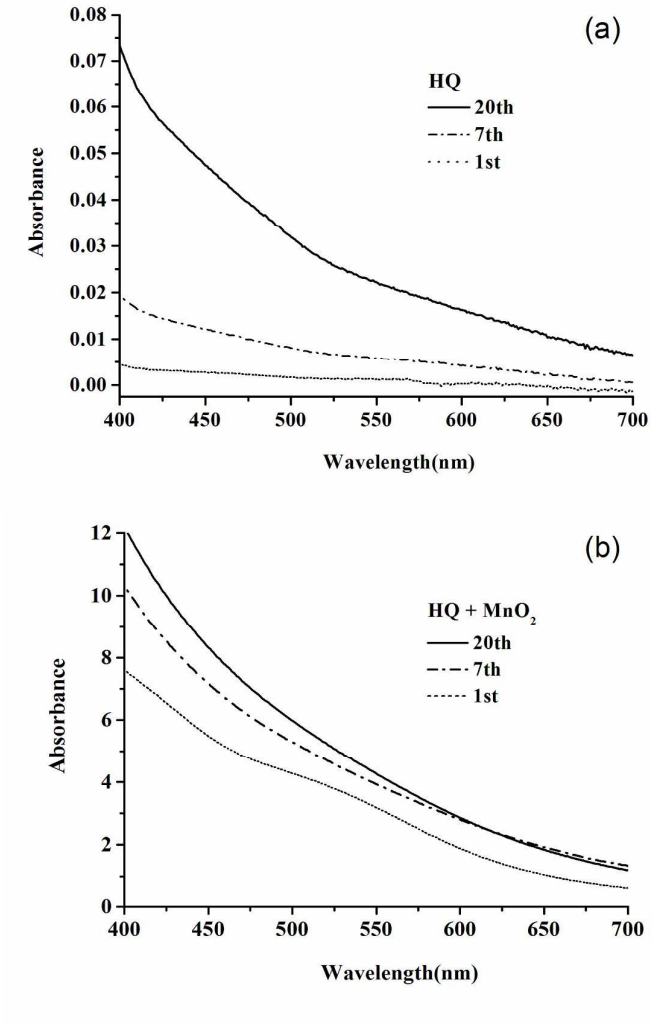

Fig. 1

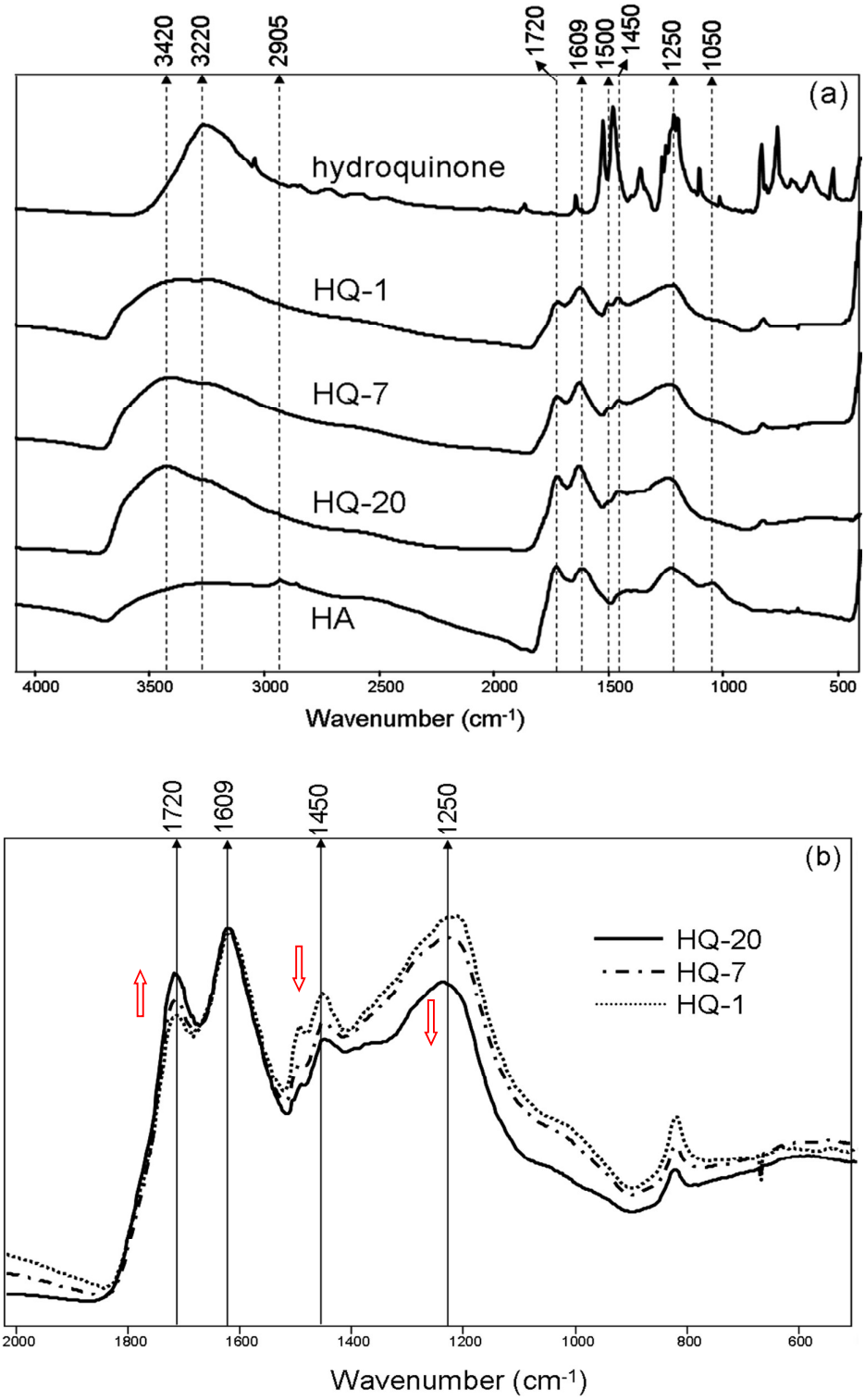

Fig. 2

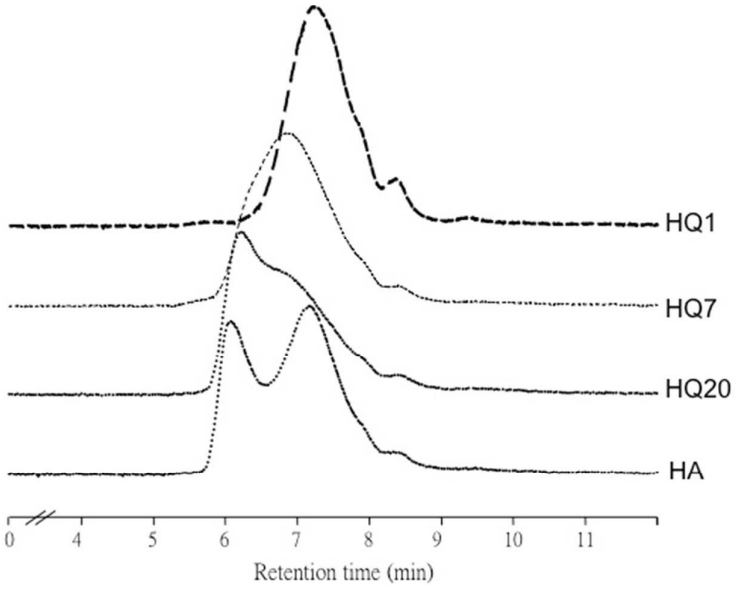

Fig. 3

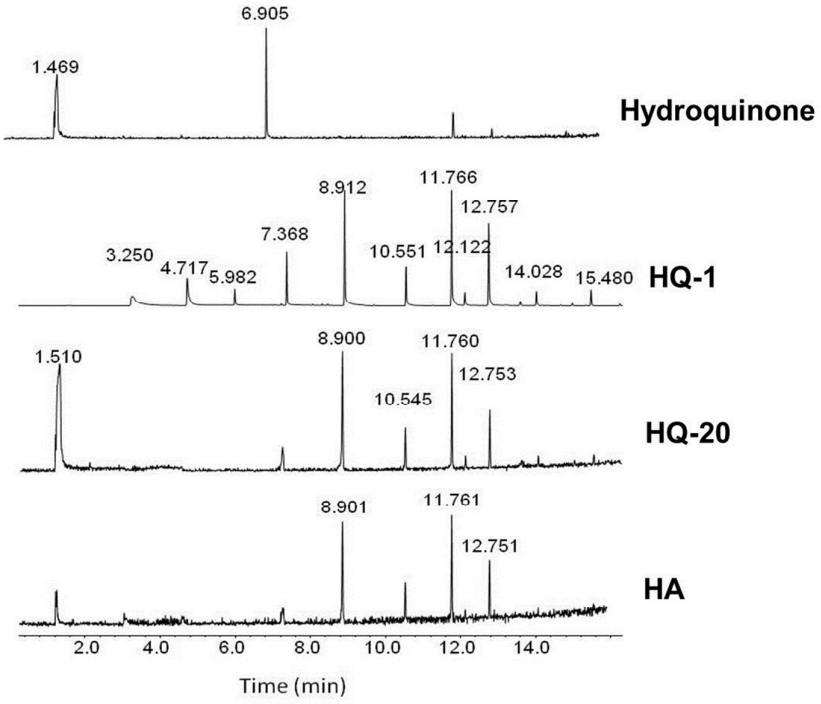

Fig. 4

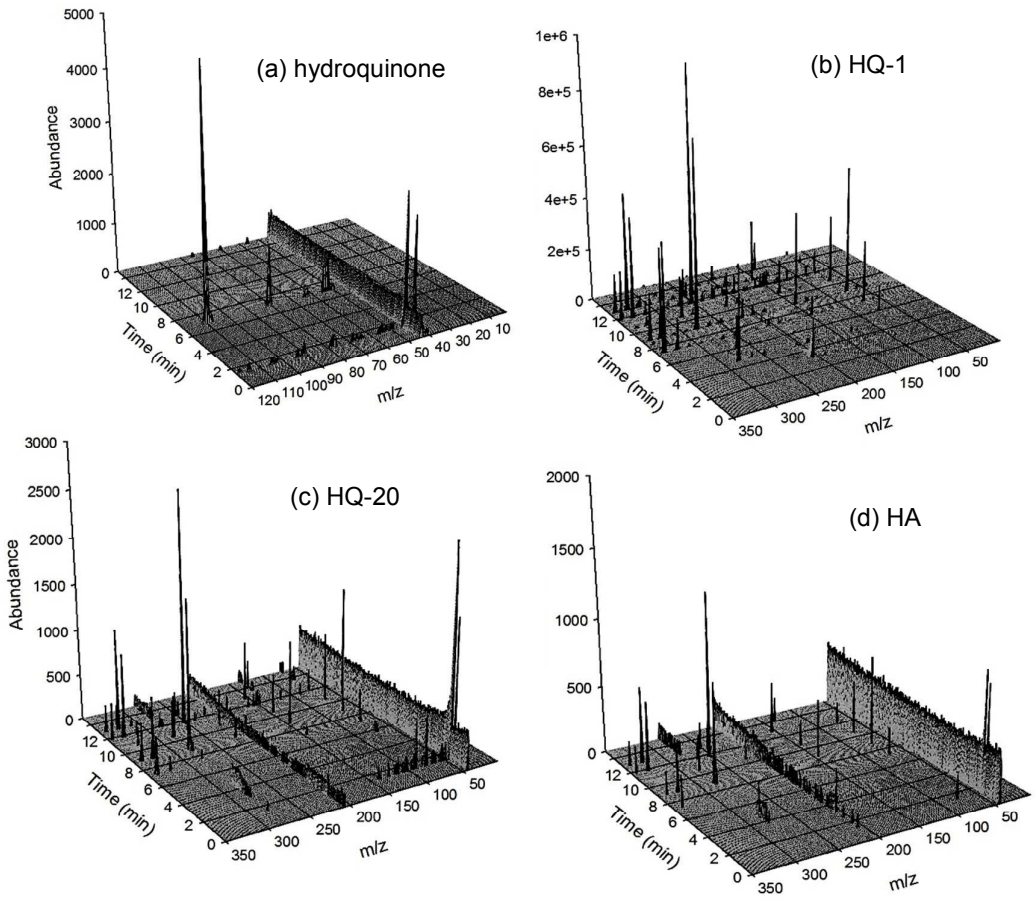

Fig. 5

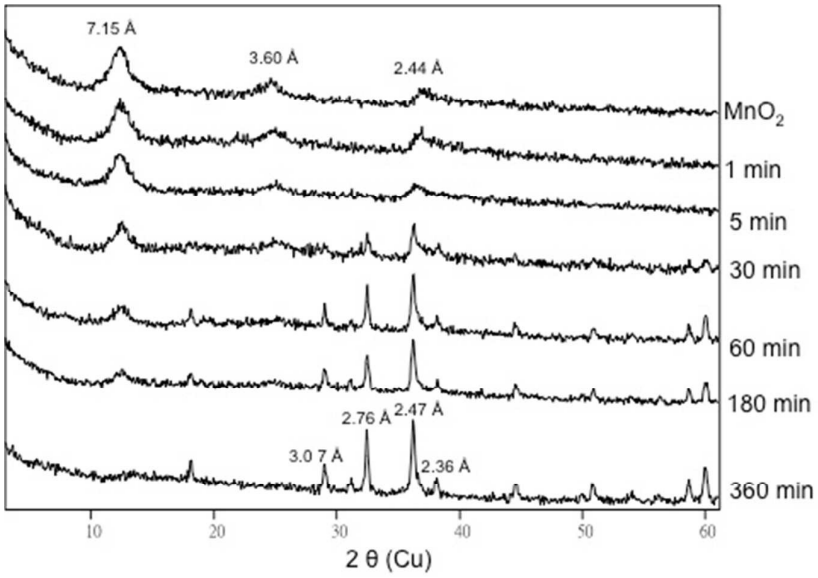

Fig. 6

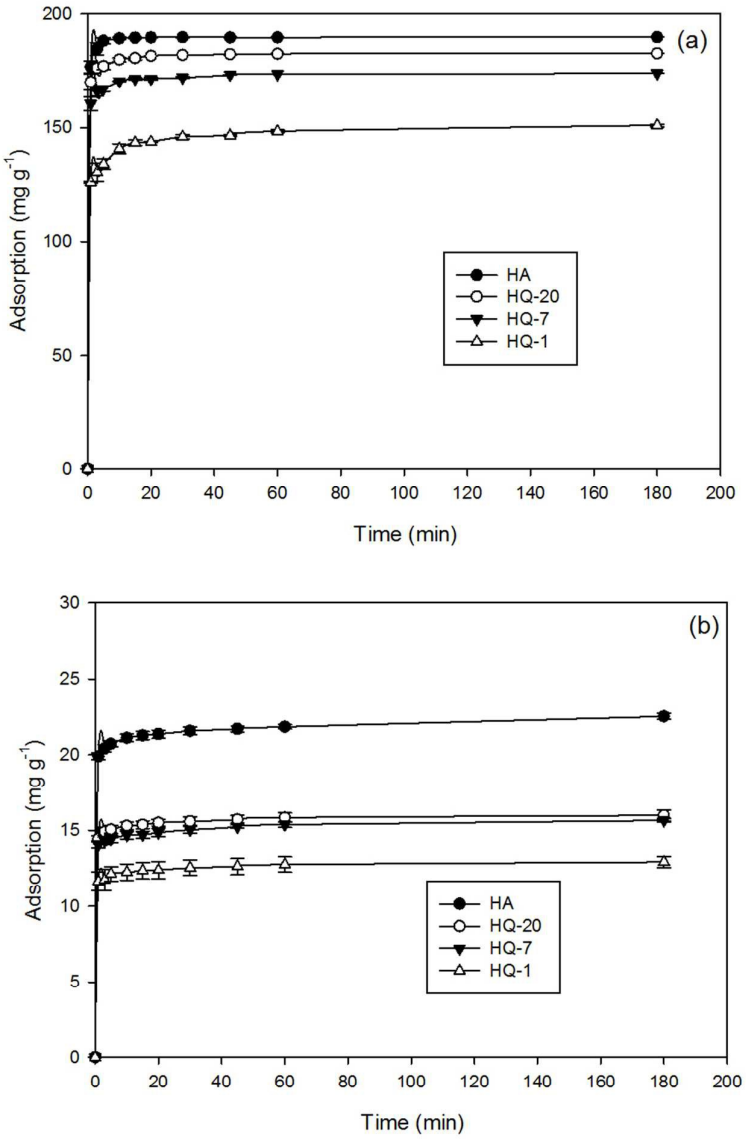

Fig. 7

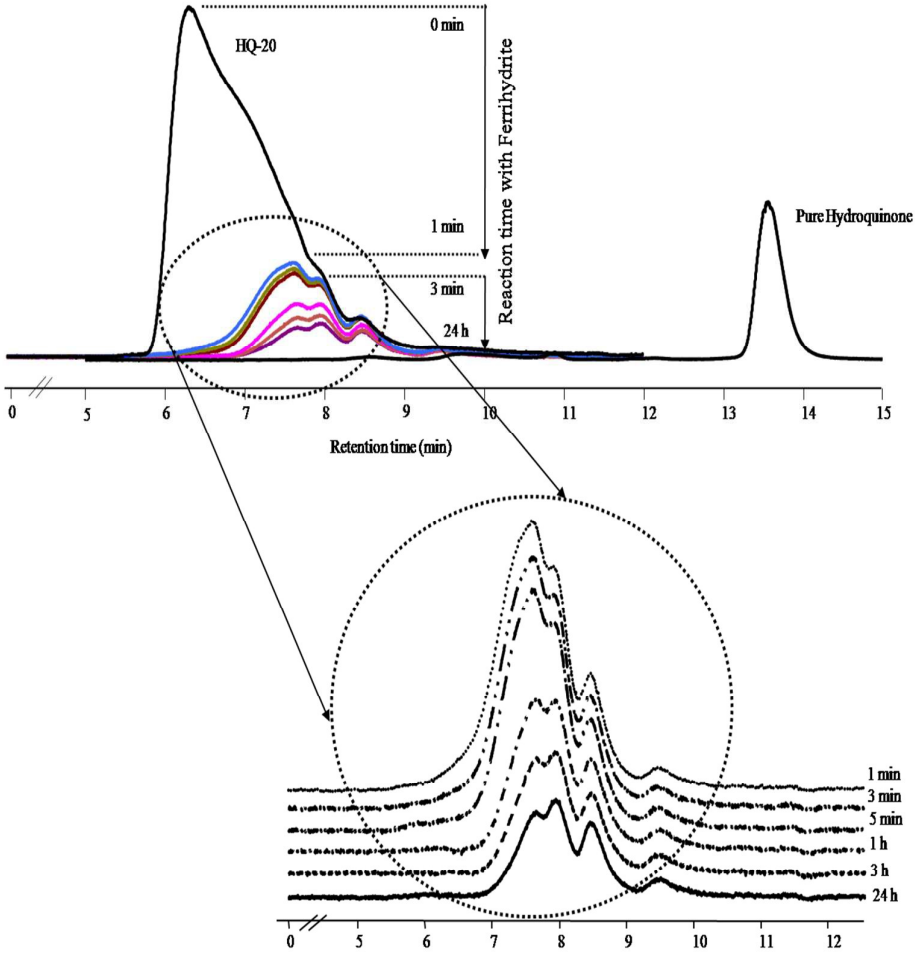

Fig. 8

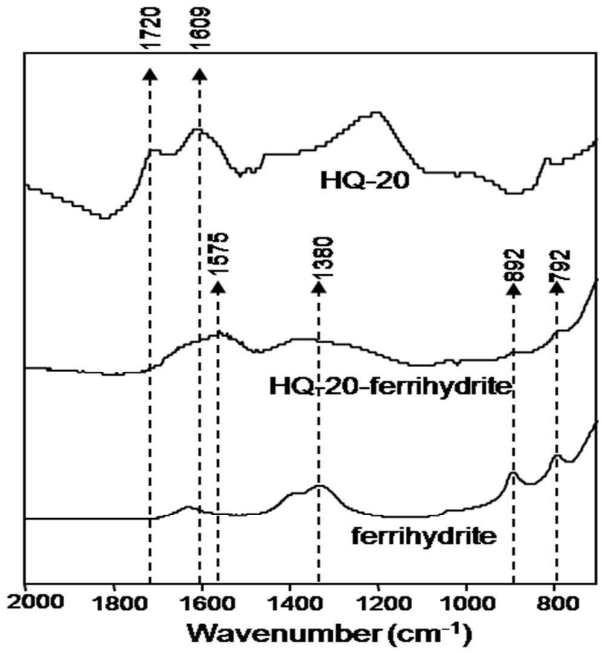

Fig. 9

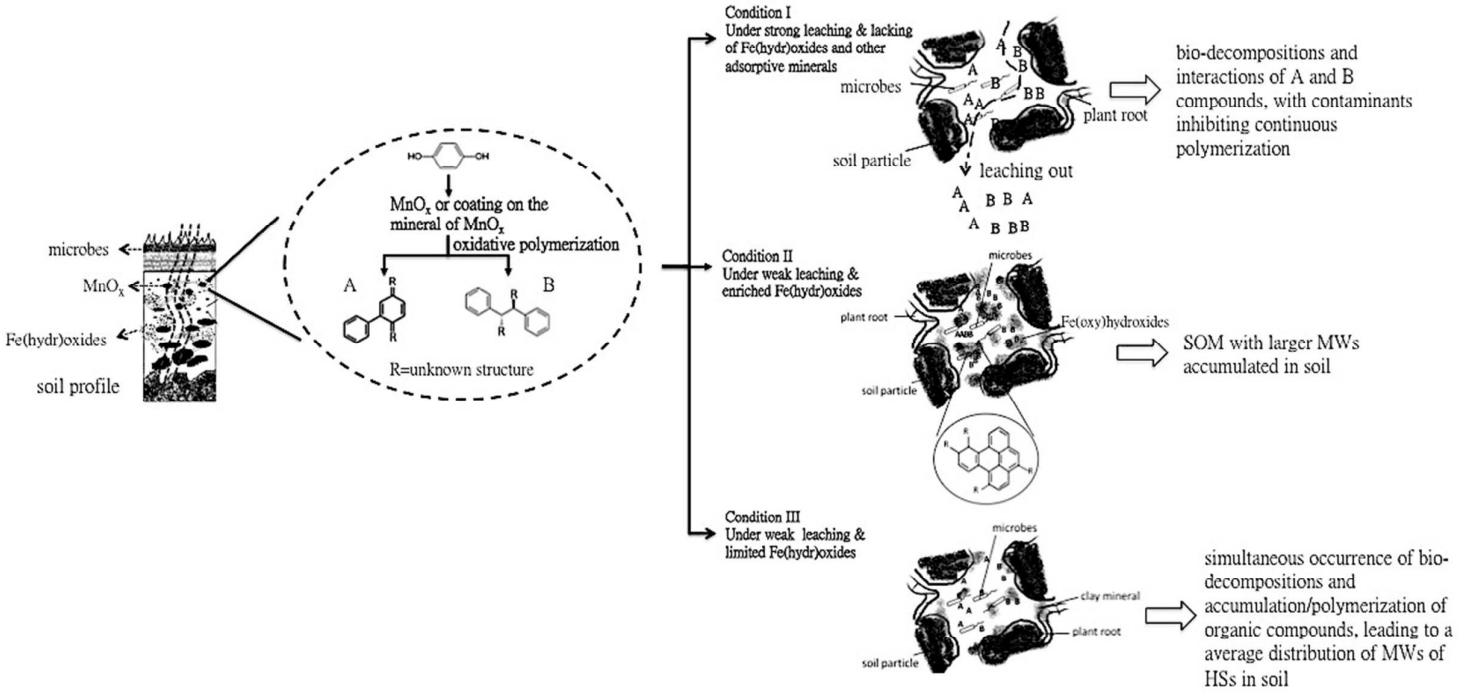

Fig. 10

Table 1

Elemental composition (%) of HQ samples derived from the browning reaction and comparisons with HA

	Proportion (%) of total weight				
Adsorbent	N	C	H	O	H/C[a]
HA	2.5	54.9	4.2	38.2	0.9
Hydroquinone	0.1	65.4	5.3	28.2	-
HQ-1	0.1	54.8	3.4	40.2	0.7
HQ-7	0.1	56.6	3.3	40.1	0.7
HQ-20	0.1	54.9	3.4	41.5	0.8

[a] Atomic ratio.

Table 2

GC-MS peaks of HQ samples and HA identified by NIST Library

Peak time (min)	Compounds	Major (m/z)
1.469	acetaldehyde[1]	44
3.250	methyl-phenylindole[2], 1-benzopyrylium,2-phenyl[2]	207
4.717	benzo-phenothiazine-dioxide[2]	281
5.982	salicylic acid[2]	282
	4-hydroxymandelic acid[2], ethyl ester[2]	340
6.905	hydroquinone[1], 1,4-Benzenediol[1]	110
7.368	3,5,7-trimethoxy-2-(4-methoxyphenyl)-/benzopyran[2]	342
	10-ethyl-8-phenyl[2], Tetrahydro-dimethoxybenzo[2]	341
8.912/8.900	benzoic acid/ hydroxyl-methylphenyl[2,3,4]	296
	benzofuran[2,3,4]	310
	siloxane/nonamethylpentasiloxane[4]	340
11.766/11.760	dihydrobenzo(E)pyrene[2,3,4]	254
	quinolinone/ 3-hydroxy-4-(3-hydroxyphenol)- [4]	253
	cyclopentadienebutanenitrile[4]	253
	androstan[4]	346
12.757/12.753	14-ethenyl-7,8-dihydro[2,3,4]	327
	naphtho-cyclodeca-biphenylene[4]	328
14.028[2]	2-methoxybenzoylformic acid[2], pentamethyl phenyl-[2]	135
15.480[2]	pentamethyl phenyl-[2]	135

[1] peak of compound from the hydroquinone

[2] peak of compound from the HQ-1

[3] peak of compound from the HQ-20

[4] peak of compound from the HA

Table 3

First and second order regressions for adsorption kinetics

	First-order		Second-order	
Ferrihydrite	k (min^{-1})	R^2	k $(mg\ L^{-1})^{-1}\ min^{-1}$	R^2
HQ-1	2.3×10^{-2}	0.90	2×10^{-3}	0.92
HQ-7	5.3×10^{-2}	0.86	2.4×10^{-2}	0.92
HQ-20	5.8×10^{-2}	0.89	3×10^{-2}	0.97
HA	7.6×10^{-2}	0.70	5.8×10^{-2}	0.83
Goethite				
HQ-1	1.2×10^{-3}	0.79	7×10^{-5}	0.80
HQ-7	1.4×10^{-3}	0.88	7×10^{-5}	0.88
HQ-20	1.6×10^{-3}	0.82	8×10^{-5}	0.82
HA	3.0×10^{-3}	0.84	2×10^{-4}	0.84